

Developing almond shell-derived activated carbons as CO₂ adsorbents

M.G. Plaza, C. Pevida, C.F. Martín, J. Feroso, J.J. Pis, F. Rubiera *

Instituto Nacional del Carbón, CSIC, Apartado 73, 33080 Oviedo, Spain

Abstract

Two series of carbon dioxide adsorbents were prepared from almond shells, by carbonisation followed either by activation with CO₂ or by heat treatment in the presence of ammonia gas (amination). Both procedures gave carbons with high CO₂ adsorption capacities in pure CO₂ as well as in a binary mixture of 15 % CO₂ in N₂. Activation with carbon dioxide significantly developed porosity in the samples, mostly in the micropore domain, while amination at 800 °C moderately developed narrow microporosity in the char and incorporated stable nitrogen functionalities, which enhanced CO₂ selectivity. Amination showed two additional advantages over conventional activation with CO₂: a greater carbon yield and a shorter soaking time.

Keywords: Adsorption; CO₂ capture; Activated carbon; Amination

1. Introduction

It is widely accepted that CCS, carbon dioxide capture and storage, will be necessary to satisfy the energy demand without contributing to global warming in the forthcoming years, while alternatives to fossil fuels are developed. Adsorption is one of the technologies that can be applied to carry out the separation of CO₂ (capture step).

Among all adsorbents, activated carbons present a series of advantages as CO₂ adsorbents: high adsorption capacity, ease of regeneration, low cost, and insensitiveness to moisture.

Almond shells are a low-cost, relatively abundant agricultural by-product, that can be used as a feedstock for the production of microporous activated carbons through a first

* Corresponding author. Fax: +34 985297662
E-mail address: frubiera@incar.csic.es (Fernando Rubiera)

step of carbonisation followed by activation with CO₂ [1-3]. The adsorption capacity of an activated carbon is mainly governed by its texture but it is also strongly influenced by the surface chemistry. The presence of nitrogen functionalities on the carbon surface have been reported in the past to be effective towards the adsorption of acid gases, such as H₂S and SO₂ [4, 5]. Attention has also been given to the introduction of nitrogen functionalities into the carbon for enhancing the CO₂ adsorption capacity [6-12].

Among other possibilities, nitrogen can be introduced into the carbon matrix by reaction with gaseous ammonia [13-19]. Ammonia can react with surface oxides and active sites present at the edges of the graphene layers to form amines, amides, imides, lactams, nitriles, pyridine- or pyrrole-like functionalities [14, 15, 19-21].

In this work two different approaches for developing efficient carbon dioxide adsorbents are compared: conventional activation with carbon dioxide, and heat treatment with gaseous ammonia, from now on referred to as amination. The main objective of amination is the introduction of basic nitrogen functionalities, while the focus of activation is texture development. In both cases, the final aim is to enhance CO₂ adsorption.

2. Experimental

Raw almond shells were ground and sieved, and a particle size between 1 and 3 mm was selected for further treatment. A first step of carbonisation was carried out at 600 °C in N₂ flow up to an average char yield of 24 %. The resulting char was denoted as A. A first series of samples were prepared by conventional activation of the char with 10 cm³ min⁻¹ of carbon dioxide at 700 °C to obtain different burn off degrees: 20, 40 and 50 %. The samples will be referred to as AA720, AA740 and AA750, respectively.

A second series of samples were obtained by treating the char with $50 \text{ cm}^3 \text{ min}^{-1}$ of ammonia gas for 2 h at four different temperatures: 400, 600, 800 and 900 °C. These samples will be denoted as AN400, AN600, AN800 and AN900, respectively.

The chemical characterisation of the samples involved proximate and ultimate analyses, estimation of the pH_{PZC} (point of zero charge) and Temperature Programmed Desorption tests (TPD). Proximate analysis was carried out in a LECO TGA-601. The carbon, hydrogen, and nitrogen contents were determined using a LECO CHN-200, and the sulfur and oxygen content in a LECO S-144-DR and a LECO VTF-900, respectively. Estimation of the point of zero charge was accomplished by a mass titration method adapted from Noh and Schwarz [22]. It involves the measurement of the pH of carbon suspensions in distilled water, once the equilibrium was attained. Different carbon contents were used, up to 20 wt.%. The free space of the test tube was filled with nitrogen, and the suspensions were continually stirred at room temperature. The TPD tests were carried out in a thermogravimetric analyser coupled to a FTIR spectrometer. A flowrate of $50 \text{ cm}^3 \text{ min}^{-1}$ of Ar and a heating rate of 15 °C min^{-1} up to a maximum temperature of 1000 °C were used.

All the samples were characterised by physical adsorption of N_2 and CO_2 at -196 °C and 0 °C, respectively, in a volumetric apparatus, TriStar 3000, from Micromeritics®. Prior to the adsorption measurements, the samples were outgassed overnight at 100 °C under vacuum. The use of both adsorbates gave complementary information: the adsorption of CO_2 at 0 °C and up to 1 bar is restricted to pores narrower than 1 nm, whereas N_2 adsorption at -196 °C covers wider pore sizes but presents diffusion limitations in the narrowest pores. S_{BET} (apparent surface area) of the samples was evaluated from the N_2 adsorption isotherms by the BET equation. V_{P} (total pore volume) was assessed from the amount of adsorbed nitrogen at a relative pressure of 0.99. V_{DR} (micropore volume)

and W_0 (narrow micropore volume; pore width below 0.7 nm) were estimated by the Dubinin-Radushkevich method, from the N_2 and CO_2 adsorption isotherms, respectively.

The CO_2 capture capacity of the adsorbents was evaluated in a Setaram TGA 92 thermogravimetric analyser, which recorded the mass uptake of the samples when exposed to a gas stream containing CO_2 . Prior to the CO_2 adsorption tests, samples were dried in Ar at 100 °C for 1h. Further details can be found elsewhere [6].

3. Results and discussion

3.1. Chemical characterisation

Table 1 presents the chemical analysis of the obtained carbons. The raw almond shells present low ash and sulphur content, thus being a good precursor for obtaining activated carbons. After the carbonisation step, the char presents a carbon content above 90 %, no sulphur and still relatively low ash content. The oxygen content was substantially reduced during the carbonisation step as it is associated to the volatile matter of the biomass (mainly constituted by cellulose and hemicellulose). However, the char still presents noticeable oxygen content that can play an important role in adsorption processes and also in the surface reactions with ammonia.

Amination incorporated nitrogen into the carbon matrix throughout the studied temperature range, reaching a maximum of 4.5 wt. % at 800 °C. This nitrogen content is relatively high, taking into account that the chars have not been subjected to oxidation prior to the ammonia treatment, as it is customary [18, 20]. The absence of an oxidation treatment with concentrated acids is an added advantage of the methodology presented in this work, as it simplifies the production process of the carbons. Moreover, the aminated carbons still present noticeable amounts of oxygen that can provide interesting

properties to the adsorbents, such as a higher reactivity, polarity, and electrical conductivity[23].

Carbonisation results in an increase of the pH_{PZC} , from 7 to 9, as a consequence of the loss of surface functionalities. This basicity may come from basic surface oxides formed, upon exposure to air, in the active sites generated during the heat treatment [21, 24], but also from non-heteroatomic Lewis base sites, characterised by regions of π electron density on the carbon basal planes [25]. Activation with carbon dioxide increases the basicity of the carbons, according to the shift in pH_{PZC} . This can be partly a consequence of the extended heat treatment at a temperature higher than that of the carbonisation step, but also of the formation of basic pyrone-type functionalities during the activation process [26, 27]. Notice that sample AA750 presents higher oxygen content than the starting char, A. Amination produced even more basic carbons, with pH_{PZC} up to 12, due to the incorporation of basic nitrogen functionalities.

To study the nature of the functional groups present on the surface of the samples, temperature programmed desorption tests were carried out. The corresponding CO_2 and CO evolution profiles analysed by the FTIR are depicted in Figure 1; only one sample of the AA7 series has been included for illustrative purposes, taking into account the likeness of the TPD profiles between activated samples. For comparative purposes, the IR absorbed intensity has been normalised by the mass of sample used (*ca.* 20 mg). The starting char, A, presents CO_2 evolution with maxima at 400 and 690 °C. Although CO_2 evolution in that temperature range is commonly assigned to decomposition of carboxyls and lactones, the DRIFT (diffuse reflectance infrared Fourier transform) spectrum of A (Figure 2) does not show the characteristic band in the nearby of 1700 cm^{-1} . However, it does present a sharp band at 1600 cm^{-1} and a group of overlapping bands between 1100 and 1500 cm^{-1} that have been related to carboxyl-

carbonate structures [28, 29]. AA750 presents CO₂ evolution at lower temperature, with maximum at 145 °C, which might come from the decomposition of labile carboxyls formed upon exposure to air after the activation process [30]. Aminated samples present lower CO₂ emissions than the starting char, A, due to the heat treatment and also to the surface reactions with ammonia.

The starting char, A, presents CO evolution with maximum at 740 °C, see Figure 1b, which may come from the decomposition of ethers, phenols and carbonyls. Sample AA750 presents CO evolution at higher temperatures, with maximum at 900 °C, which probably come from the decomposition of pyrone groups formed upon activation with carbon dioxide [31]. Aminated samples present lower CO emissions than the starting char, mainly due to the surface reactions with ammonia, taking into consideration the high thermal stability of the CO-evolving groups.

With the exception of AN600, emissions of HCN and NH₃ were almost negligible. Therefore, AN800 and AN900, which present the highest nitrogen contents of the series, have nitrogen functionalities that are stable to heating up to 1000° C, *i.e.* pyridine type [6]. AN600 presents HCN and NH₃ emissions (see Figure 3) with maxima at 800 °C, and 700-750 °C, respectively, that might come from the decomposition of amides and lactams [20].

3.2. Textural characterisation

The starting char presents only incipient microporosity, not accessible to N₂ molecules at -196 °C, due to diffusion limitations. All the samples present type I nitrogen adsorption isotherms (see Figure 4a), characteristic of microporous materials.

Activation with carbon dioxide develops substantially the texture of the starting char, leading to carbons with BET surface areas up to 1090 m² g⁻¹ and total pore volumes up to 0.50 cm³ g⁻¹ (see Table 2). As the burn off increases, the pore volume is gradually

developed at the expense of a reduction in the final carbon yield. In Table 2 a progressive widening of L_{DR} (micropore width) with carbon dioxide activation can also be seen.

Amination at temperatures above 600 °C also develops the porous structure of the char although to a lesser extent than activation with carbon dioxide. To study the effect of heat treatment over the texture development of the char, a sample was prepared by heating the char, A, in 50 cm³ min⁻¹ of N₂ flowrate at 800 °C for 2 h. This sample, called A800, presents very narrow microporosity, with N₂ diffusion limitations at -196 °C (see Table 2). On the other hand, AN800 is a highly microporous carbon with slightly wider micropores, accessible to N₂ at -196 °C. Ammonia is known to decompose at high temperatures, producing atomic H and NH₂ and NH free radicals that react with the carbon releasing gaseous H₂, CH₄, HCN and (CN)₂ [13, 17], developing the narrow microporosity of the char.

Figure 4b represents the CO₂ adsorption isotherms of the samples at 0 °C. The shape of the isotherms of the activated samples tends to be more rectilinear as the burn off increases. This is due to a progressive widening of the micropore size with the extent of activation. From the CO₂ isotherms of the aminated samples, it can be seen that creation of new microporosity (narrower than 1 nm) is maximum at 800 °C. Below that temperature, the CO₂ isotherms of the starting char and the aminated samples at 400 and 600 °C are almost coincident, and above 800 °C, gasification is so severe that the narrow micropore volume is reduced due to the collapse of adjacent pore walls. If the narrow micropore volume (W_0), obtained from the CO₂ isotherms, is compared with the total pore volume, obtained from the N₂ isotherms (V_p), it can be seen that the latter is smaller for the aminated samples, with the exception of sample AN900. This is due to

the existence of diffusion limitations to the entrance of N₂ molecule at -196 °C in narrow micropores. Thus, the porosity created by amination is very narrow.

3.3. CO₂ capture

Figure 5a summarises the CO₂ capture capacities of the samples at 25 °C and 100 °C obtained at 1 bar in 50 cm³ min⁻¹ of pure CO₂ flow, by means of a thermogravimetric analyser. The CO₂ capture capacities at 25 °C of two commercial activated carbons, C and R, have been included for comparison purposes; further details about these carbons can be found elsewhere [6]. As expected for any physisorption processes, the adsorption capacity of the carbons decreases with increasing temperature.

All the activated samples present higher CO₂ capture capacity than that of the starting char at both temperatures, due to the substantial texture development produced during carbon dioxide activation. Moreover, the CO₂ capture capacity at 25 °C reaches its maximum value, 11.7 wt. %, for sample AA750. This capture capacity is above that of the commercial activated carbons. Even at 100 °C, the samples still present significant capacities, up to 4.1 wt. %. Comparing these results with those of a previous work from our group [32], it has been found that for the same burn off (and very close textural development), and the same starting char, A, activation at 700 °C results more effective than at 800 °C, when the aim is to maximise CO₂ adsorption at atmospheric pressure.

Amination, on the other hand, does not always result in an increase in the CO₂ adsorption capacity of the char, despite the introduction of nitrogen functionalities. The best result was obtained for the sample aminated at 800 °C, in good agreement with previous results [6, 27]. This sample is also the carbon with the highest nitrogen content and the highest narrow micropore volume among the aminated samples presented in this work. The CO₂ capture capacity of AN800 lies between that of AA720 and AA740,

although its porous volume is significantly lower. Therefore, ammonia treatment seems to be playing an enhancement effect in the adsorption of CO₂.

In an attempt to study the effect of the nitrogen functionalities over CO₂ adsorption, sample AN800 was subjected to heat treatment at 800 °C in 50 cm³ min⁻¹ of N₂ flow. The resultant carbon was denoted as AN800P. The nitrogen content was only slightly reduced by the heat treatment, due to the high thermal stability of the N-functionalities introduced during amination at 800 °C. As can be seen from Table 2, post-amination heat treatment widened the microporosity of the sample. As a result, microporosity in AN800P results more accessible to N₂ at -196 °C. The CO₂ adsorption capacity of AN800P is slightly lower than that of AN800 (Figure 5a), despite the higher pore volume of AN800P, probably due to the small reduction in the nitrogen content.

Figure 5b presents the CO₂ adsorption capacity of samples AA740, AA750 and AN800 at 25 °C and 1 bar in a flowrate of 30 cm³ min⁻¹ of a gas stream containing 15 % of CO₂ in N₂. These tests were carried out to evaluate the performance of selected adsorbents in a binary mixture containing N₂ and CO₂, in a ratio that simulated that of a flue gas stream. As expected, the attained adsorption capacity is lower than in pure CO₂ flow, due to the diminished partial pressure of CO₂. However, the samples still present a significant adsorption capacity. Moreover, the difference between the adsorption capacity of AN800 and that of the activated samples becomes smaller when CO₂ partial pressure diminishes, indicating that amination enhances CO₂ selectivity. This is a promising result for postcombustion capture applications where low CO₂ partial pressures are involved. Currently, CO₂ adsorption-desorption cyclic tests under more realistic conditions are being conducted in a purpose-built lab-scale fixed bed reactor. Thus, amination at 800 °C is proposed here as an alternative pathway to conventional activation with carbon dioxide for the production of carbon-based CO₂ adsorbents.

Carbons with similar CO₂ capacities can be obtained, with the added advantages of greater carbon yield (see Table 2) and shorter treatment times (2 vs. 5-45 h). Similar findings have been observed in our group departing from a different biomass by-product [27].

4. Conclusions

Basic activated carbons with a CO₂ adsorption capacity at 25 °C up to 11.7 wt. %, in pure CO₂ flow, and up to 5.2 wt. %, in a binary mixture of 15 % CO₂ in N₂, have been obtained from low-cost biomass by-products, through conventional activation with carbon dioxide.

Amination is proposed as an alternative pathway to conventional activation with carbon dioxide, for producing effective CO₂ adsorbents. Nitrogen was successfully incorporated into the carbon structure without the need of a previous oxidation step. The effect of the temperature of the amination treatment has been studied, and 800 °C has been proven as the optimum temperature, as CO₂ adsorption capacity and nitrogen incorporation reached the maximum values. Aminated carbons achieved CO₂ capture capacities at 25 °C up to 9.6 wt. % in pure CO₂ flow, and up to 4.8 wt. % in a binary mixture of 15 % of CO₂ in N₂. Compared to activation with carbon dioxide, amination has additional advantages: greater carbon yields and shorter soaking times.

Acknowledgements

This work was carried out with financial support from the Spanish MICINN (Project ENE2008-05087). M.G.P., C.F.M. and J.F. acknowledge funding from the CSIC I3P and, JAE programs, co-financed by the European Social Fund, and PCTI Asturias, respectively.

References

- [1] F. Rodríguez-Reinoso, J.d.D. López-González, C. Berenguer, *Carbon* 20 (1982) 513-518
- [2] F. Rodríguez-Reinoso, J.d.D. López-González, C. Berenguer, *Carbon* 22 (1984) 13-18
- [3] A. Linares-Solano, J.d.D. López-González, M. Molina-Sabio, F. Rodríguez-Reinoso, *Journal of Chemical Technology and Biotechnology* 30 (1980) 65-72
- [4] F. Adib, A. Bagreev, T.J. Bandosz, *Langmuir* 16 (2000) 1980-1986
- [5] A. Bagreev, S. Bashkova, T.J. Bandosz, *Langmuir* 18 (2002) 1257-1264
- [6] C. Pevida, M.G. Plaza, B. Arias, J. Feroso, F. Rubiera, J.J. Pis, *Applied Surface Science* 254 (2008) 7165-7172
- [7] M.G. Plaza, C. Pevida, B. Arias, J. Feroso, A. Arenillas, F. Rubiera, J.J. Pis, *Journal of Thermal Analysis and Calorimetry* 92 (2008) 601-606
- [8] M.G. Plaza, C. Pevida, A. Arenillas, F. Rubiera, J.J. Pis, *Fuel* 86 (2007) 2204-2212
- [9] T.C. Drage, A. Arenillas, K.M. Smith, C. Pevida, S. Piippo, C.E. Snape, *Fuel* 86 (2007) 22-31
- [10] M.M. Maroto-Valer, Z. Lu, Y. Zhang, Z. Tang, *Waste Management* 28 (2008) 2320-2328
- [11] M.M. Maroto-Valer, Z. Tang, Y. Zhang, *Fuel Processing Technology* 86 (2005) 1487-1502
- [12] J. Przepiórski, M. Skrodzewicz, A.W. Morawski, *Applied Surface Science* 225 (2004) 235-242
- [13] H.P. Boehm, G. Mair, T. Stoehr, A.R. De Rincon, B. Tereczki, *Fuel* 63 (1984) 1061-1063

- [14] B.J. Meldrum, C.H. Rochester, *J. Chem. Soc., Faraday Trans.* 86 (1990) 861-865
- [15] B. Stohr, H.P. Boehm, R. Schlögl, *Carbon* 29 (1991) 707-720
- [16] S. Biniak, G. Szymanski, J. Siedlewski, A. Swiatkowski, *Carbon* 35 (1997) 1799-1810
- [17] K.B. Bota, G.M.K. Abotsi, *Fuel* 73 (1994) 1354-1357
- [18] R.J.J. Jansen, H. van Bekkum, *Carbon* 32 (1994) 1507-1516
- [19] P. Vinke, M. van der Eijk, M. Verbree, A.F. Voskamp, H. van Bekkum, *Carbon* 32 (1994) 675-686
- [20] R.J.J. Jansen, H. van Bekkum, *Carbon* 33 (1995) 1021-1027
- [21] K.A. Grant, Q. Zhu, K.M. Thomas, *Carbon* 32 (1994) 883-895
- [22] J.S. Noh, J.A. Schwarz, *Journal of Colloid and Interface Science* 130 (1989) 157-164
- [23] R.C. Bansal, M. Goyal, *Activated carbon adsorption*, CRC Press, Boca Raton, FL, 2005
- [24] E. Papirer, S. Li, J.-B. Donnet, *Carbon* 25 (1987) 243-247
- [25] T.J. Bandoz, C.O. Ania, in: T.J. Bandoz (Ed.), *Activated carbon surfaces in environmental remediation*, Amsterdam, Elsevier Ltd., 2006
- [26] F. Carrasco-Marin, E. Utrera-Hidalgo, J. Rivera-Utrilla, C. Moreno-Castilla, *Fuel* 71 (1992) 575-578
- [27] M.G. Plaza, C. Pevida, B. Arias, J. Feroso, M.D. Casal, C.F. Martín, F. Rubiera, J.J. Pis, *Fuel* 88 (2009) 2442-2447
- [28] J. Zawadzki, *Carbon* 16 (1978) 491-497
- [29] C. Ishizaki, I. Martí, *Carbon* 19 (1981) 409-412
- [30] F. Rodríguez-Reinoso, A.C. Pastor, H. Marsh, A. Huidobro, *Carbon* 38 (2000) 397-406

[31] O.W. Fritz, K.J. Hüttinger, Carbon 31 (1993) 923-930

[32] M.G. Plaza, C. Pevida, B. Arias, J. Feroso, F. Rubiera, J.J. Pis, Energy
Procedia 1 (2008) 1107-1113

Tables

Table 1 Point of zero charge and chemical analysis of the samples

Sample	pH _{PZC}	Proximate analysis (% db)		Ultimate analysis (% daf)				
		VM	Ash	C	H	N	S	O
Raw A	6.7	82.3	1.3	51.4	6.1	0.3	0.6	41.6
A	9.3	13.6	4.7	91.0	2.0	0.4	0.0	6.6
AA720	9.7	11.3	4.4	93.6	0.8	0.7	0.0	4.9
AA740	9.9	12.1	5.7	91.8	0.7	0.9	0.0	6.6
AA750	10.1	11.8	10.2	90.2	0.8	1.0	0.0	8.0
AN400	9.3	7.8	5.2	91.1	1.9	1.0	0.0	6.0
AN600	11.6	6.85	5.10	88.9	1.5	3.2	0.0	6.4
AN800	10.9	3.92	4.75	89.2	0.6	4.5	0.0	5.7
AN900	12.4	3.63	5.30	90.8	0.4	4.2	0.0	4.6
AN800P	11.3	4.6	5.1	87.7	0.5	4.0	0.0	7.8

VM: volatile matter; db: dry basis; daf: dry and ash free basis

Table 2 Carbon yield and textural characterisation of the samples

Sample	Carbon yield (%)	N ₂ adsorption at -196 °C				CO ₂ adsorption at 0 °C	
		S _{BET}	V _p	V _{DR}	L _{DR}	W ₀	L ₀
		(m ² g ⁻¹)	(cm ³ g ⁻¹)	(cm ³ g ⁻¹)	(nm)	(cm ³ g ⁻¹)	(nm)
A	24	21	0.01	–	–	0.16	0.5
AA720	19	526	0.24	0.20	0.8	0.18	0.5
AA740	14	831	0.37	0.32	1.0	0.19	0.5
AA750	12	1090	0.50	0.42	1.2	0.12	0.4
AN400	23	8	0.03	–	–	0.16	0.5
AN600	23	91	0.05	–	–	0.15	0.5
AN800	21	326	0.24	0.23	0.8	0.20	0.5
AN900	18	350	0.16	0.13	1.4	0.08	0.4
A800	21	41	0.04	–	–	0.19	0.5
AN800P	19	448	0.19	0.18	1.2	0.17	0.5

S_{BET}: apparent BET surface area; V_p: total pore volume; V_{DR}: micropore volume; W₀: narrow micropore volume; L_{DR}: mean micropore width; L₀: mean narrow micropore width

Figures

Figure 1. (a) CO₂ and (b) CO evolution profiles analysed by FTIR during temperature programmed desorption tests carried out at a heating rate of 15 °C min⁻¹ up to 1000 °C in a flowrate of 50 cm³ min⁻¹ of Ar.

Figure 2. DRIFT spectrum of the starting char, A.

Figure 3. (a) HCN and (b) NH₃ evolution profiles analysed by FTIR during temperature programmed desorption tests carried out at a heating rate of 15 °C min⁻¹ up to 1000 °C in a flowrate of 50 cm³ min⁻¹ of Ar.

Figure 4. Adsorption isotherms of the prepared carbons: (a) N₂ at -196 °C and (b) CO₂ at 0°C.

Figure 5. CO₂ capture capacity evaluated in a thermogravimetric analyser at 1 bar: (a) 100 % CO₂ and (b) 15 % CO₂ in N₂.

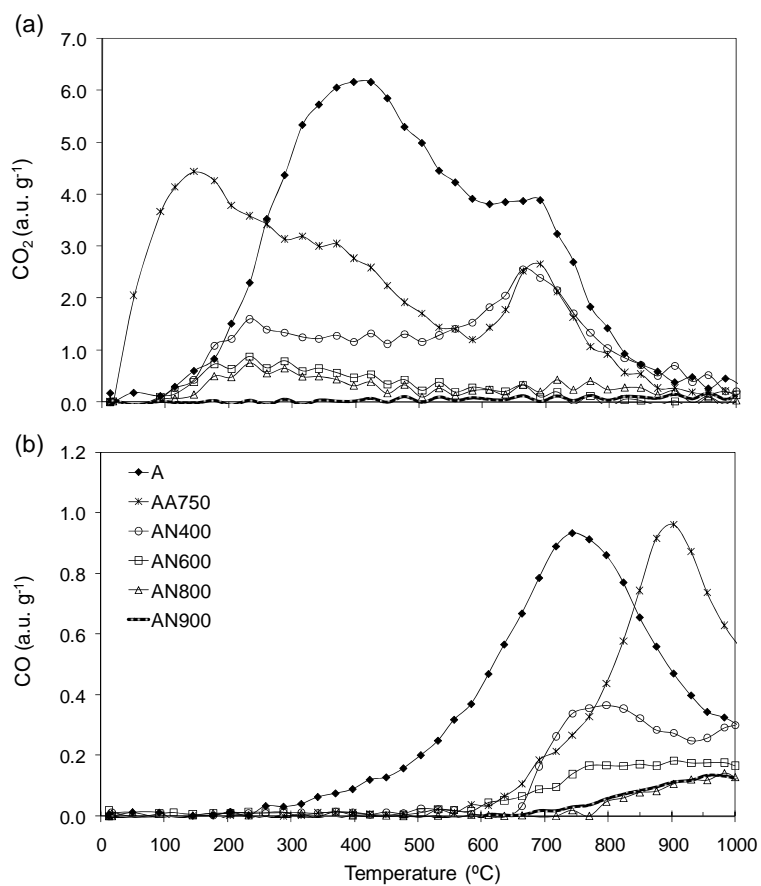


Figure 1. (a) CO₂ and (b) CO evolution profiles analysed by FTIR during temperature programmed desorption tests carried out at a heating rate of 15 °C min⁻¹ up to 1000 °C in a flowrate of 50 cm³ min⁻¹ of Ar.

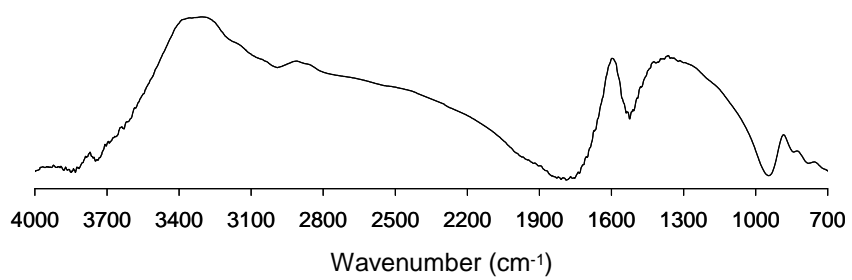


Figure 2. DRIFT spectrum of the starting char, A.

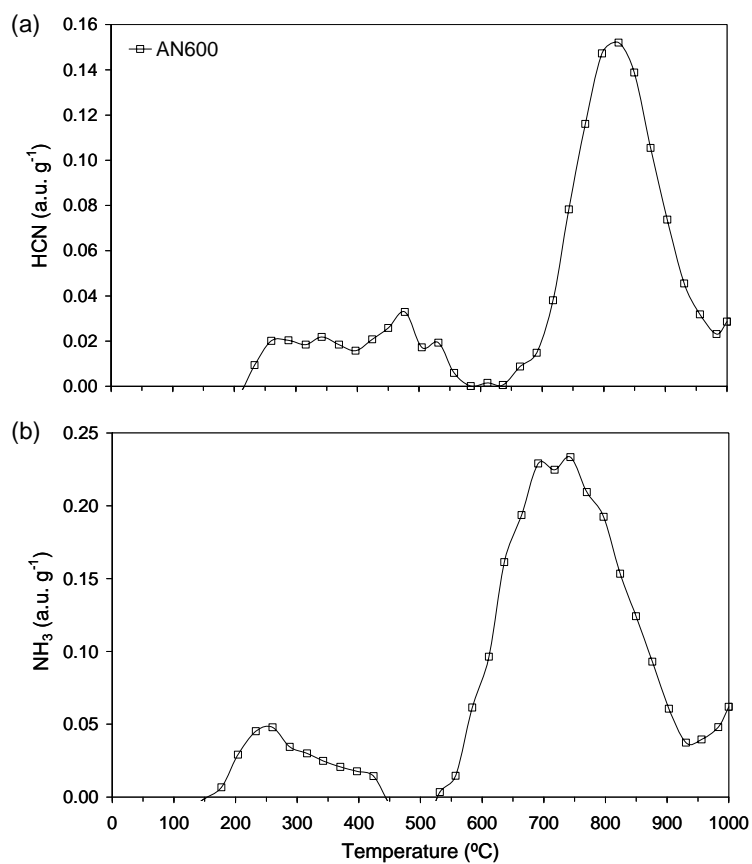


Figure 3. (a) HCN and (b) NH₃ evolution profiles analysed by FTIR during temperature programmed desorption tests carried out at a heating rate of 15 °C min⁻¹ up to 1000 °C in a flowrate of 50 cm³ min⁻¹ of Ar.

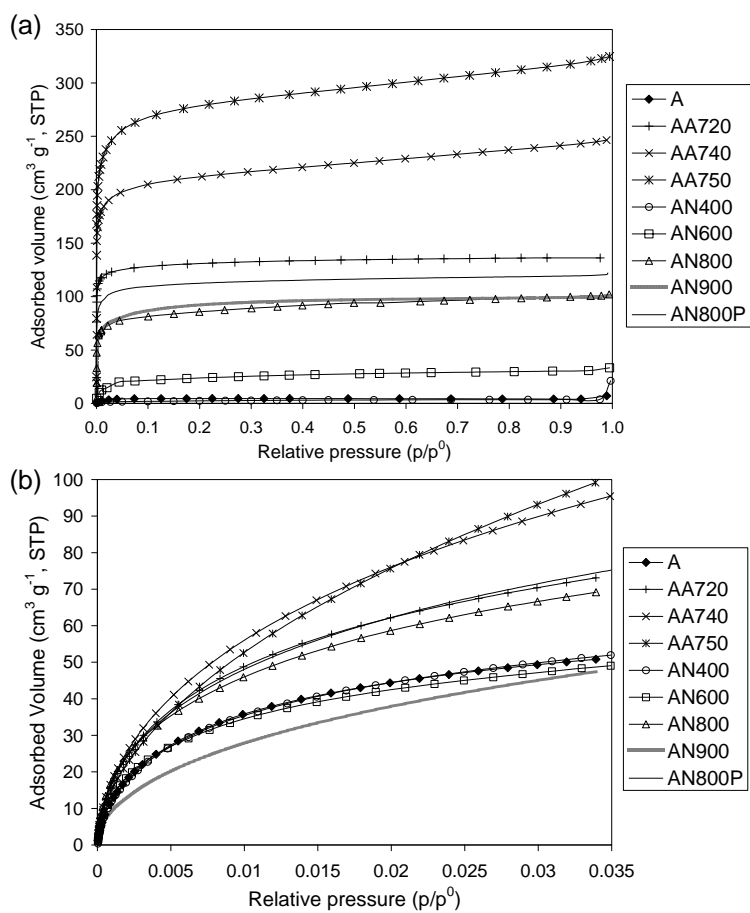


Figure 4. Adsorption isotherms of the prepared carbons: (a) N_2 at $-196\text{ }^\circ\text{C}$ and (b) CO_2 at $0\text{ }^\circ\text{C}$.

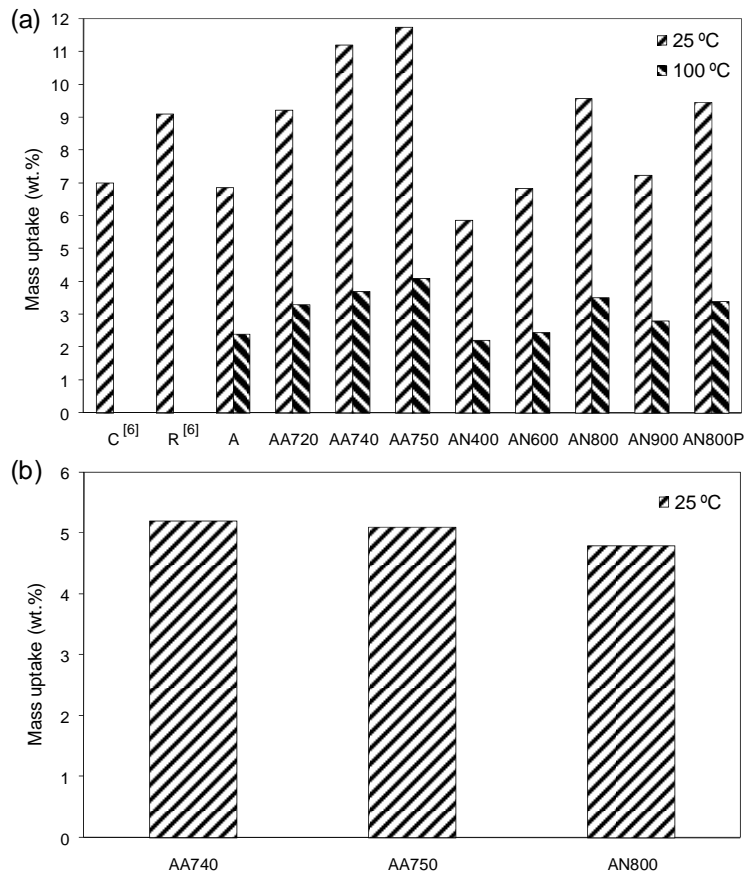


Figure 5. CO₂ capture capacity evaluated in a thermogravimetric analyser at 1 bar:

(a) 100 % CO₂ and (b) 15 % CO₂ in N₂.